Journal of Advanced Research 32 (2021) 119–131

Contents lists available at ScienceDirect

Journal of Advanced Research

journal homepage: www.elsevier.com/locate/jare

Optimal charging of fractional-order circuits with Cuckoo search

A.M. AbdelAty [a], Mohammed E. Fouda [b,c,*], Menna T.M.M. Elbarawy [a], A.G. Radwan [b,d]

[a] Engineering Mathematics and Physics Dept., Faculty of Engineering, Fayoum University, Egypt
[b] Engineering Mathematics and Physics Dept., Faculty of Engineering, Cairo University, Egypt
[c] Electrical Engineering and Computer Science Dept., University of California Irvine, Irvine, USA
[d] Nanoelectronics Integrated Systems Center (NISC), Nile University, Egypt

HIGHLIGHTS

- The differences between two main charging methodologies in FO circuits are depicted.
- The delivered charge, energy loss, and efficiency for FO circuits are studied.
- Optimal charging of three FO RC networks is obtained using compositional functional.
- Approximate solutions are reached using a prototype CPE voltage function and CS.

GRAPHICAL ABSTRACT

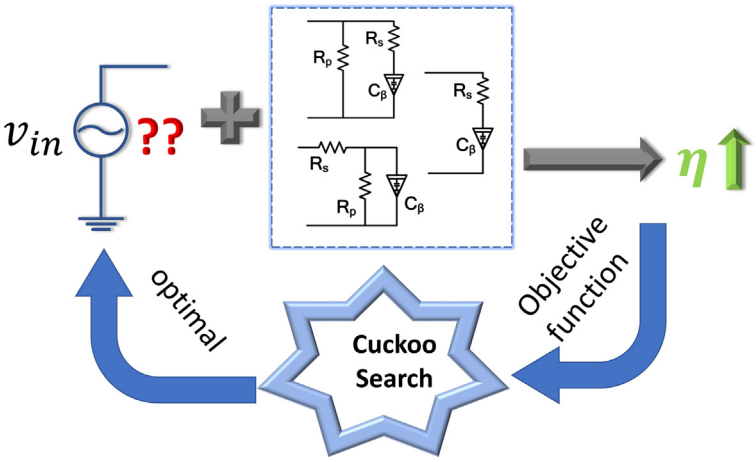

ARTICLE INFO

Article history:
Received 1 October 2020
Revised 12 November 2020
Accepted 27 November 2020
Available online 3 December 2020

Keywords:
Fractional capacitor charging
Fractional-order circuits
Optimal charging
Cuckoo search optimizer

ABSTRACT

Introduction: Optimal charging of *RC* circuits is a well-studied problem in the integer-order domain due to its importance from economic and system temperature hazards perspectives. However, the fractional-order counterpart of this problem requires investigation.
Objectives: This study aims to find approximate solutions of the most energy-efficient input charging function in fractional-order *RC* circuits.
Methods: This paper uses a meta-heuristic optimization technique called Cuckoo search optimizer to attain the maximum charging efficiency of three common fractional-order *RC* circuits. An analytical expression of the fractional capacitor voltage is suggested such that it satisfies the boundary conditions of the optimal charging problem. The problem is formulated as a fractional-order calculus of variations problem with compositional functional. The numerical solutions are obtained with the meta-heuristic optimization algorithm's help to avoid the complexities of the analytical approach.
Results: he efficiency surfaces and input voltage charging curves are discussed for fractional-order in the range $0.5 < \alpha \leq 1$.
Conclusion: The optimized charging function can approximate the optimal charging curve using at most 4 terms. The charging time and the resistive parameters have the most dominant effect on charging efficiency at constant fractional-order α.

Peer review under responsibility of Cairo University.
* Corresponding author at: Engineering Mathematics and Physics Dept., Faculty of Engineering, Cairo University, Egypt.
E-mail address: foudam@uci.edu (M.E. Fouda).

https://doi.org/10.1016/j.jare.2020.11.014
2090-1232/

Introduction

Fractional-order modeling offers better and accurate identification of the systems and has been recently used extensively to characterize many physical phenomena. Fractional-order modeling relies on the generalization of the Calculus, which is referred as fractional Calculus. The idea behind fractional calculus dates back to calculus's origins in an intriguing letter between L'Hopital and Leibniz discussing the consequences of dealing with a half order derivative. A series of contributions to the area by great mathematicians followed this letter. Examples of early contributors are Reimann, Liouville, Grunwald, Letnikov, Riesz, Caputo, and many others [1–3]. However, the fractional-calculus' theoretical development was rather slow and application-driven contributions took a lot of time to surface. It was only recently when researchers realized the advantages this modeling tool can offer. These advantages include the extra tuning knobs introduced by the new fractional-order parameter the ability to model systems with strong memory dependency due to the convolution integral involved in most of the fractional-calculus operators [4–6]. In addition, fractional-order models are compact and provide a better representation of complex systems using fewer parameters compared to their equivalent integer-order models. The application areas are ubiquitous in many science and engineering fields such as: bio-impedance modeling, chaos [7–11], control [12–14], wireless power transfer [15,16], image recognition [17], circuit theory [18–26], oscillators [27,28], modeling of energy storage devices [29–31], bio-impedance modeling [32,33], and others [34,35,11,36].

Meta-heuristic optimization algorithms have been proven to be applicable in many areas of science and engineering. They are often inspired by natural phenomena or animal behavior like hunting or flower pollination. Their working mechanism allows them to overcome notorious problems that gradient-based deterministic optimization algorithms are known to fall into, like converging to local extrema and sensitivity to the initial point of the search space. On the other hand, the search agents' stochastic movement and the random distribution of the initial population all over the search space allow meta-heuristic optimization techniques to have a higher probability of finding better solutions than traditional methods [37]. However, this comes at the cost of being more computationally demanding than traditional methods. Also, the no free lunch theorem states that there is no super meta-heuristic algorithm that can be used to solve all optimization problems [38].

Analytical solutions of fractional order problems are not always obtainable due to the complex mathematical expressions involved. So, increased interest in using meta-heuristic optimization has been recently observed in fractional-calculus literature [39,40]. Chronologically speaking, one of the earliest contributions in this field is using the differential evolution algorithm for designing a fractional order filter with a specific magnitude response [41]. Many papers followed this work in both analog and digital domains. Flower pollination algorithm (FPA) and moth flame optimizer (MFO) was used to find an infinite impulse response (IIR) approximation of digital fractional-order differential operators of orders $1/2, 1/3$, and $1/4$ [42,43]. In the analog realm, many fractional-order filters approximating polynomial based magnitude responses like Butterworth, Chebyshev, and Bessel were optimized and approximated using meta-heuristic optimization algorithms [44–50]. In this work, we use the Cuckoo Search (CS) Optimizer as it has been proven to perform better than many other meta-heuristic optimization algorithms in terms of consistency and accuracy of the obtained results specially in problems involving fractional-order models [51–53].

RC networks are basic building blocks in equivalent circuit models of energy storage devices like batteries and supercapacitors [54,55]. The maximization of energy efficiency of *RC* networks is important due to two main reasons: consuming less energy from the source to achieve the same charging target makes the system more greener, and reducing energy loss reduces thermal impacts and results in prolonging energy storage device life cycle which is important due to high price of some of the energy storage components and also the inaccessibility for maintenance of the others [56]. In integer-order circuits, the optimal charging of *RC* networks has been thoroughly discussed [57–61]. The approaches of tackling this problem ranged from optimal control [57], to the calculus of variations [58]. The conclusion is the same for the simple series *RC* circuit, that is, the source function that minimizes the loss in the resistor is the constant current input. However, this problem is still new to the area of fractional-order *RC* networks. This paper aims to find approximate solutions for the optimal charging source functions that maximize the energy efficiency for fractional-order versions of the circuits investigated in [58]. This is a continuation of the work we presented in [62] using a different objective function and more fractional-order *RC* networks.

The main objective of this paper is to find the optimal voltage charging function that maximizes the efficiency of the charging process in fractional-order *RC* circuits. The summary of contributions of this paper are as follows:

- Discuss, via a numerical study, the differences between two main charging methodologies, constant current and constant voltage, in fractional-order circuits.
- Study the delivered electric charge, energy loss, and charging efficiency for fractional-order circuits.
- Present the problem formulation of the optimal charging of three fractional-order *RC* networks using compositional functional.
- Find approximate solutions of the problem using prototype Constant Phase Element, CPE, voltage function and Cuckoo search optimizer.

The rest of this paper is organized as follows. First, an overview is provided of the concepts of fractional-calculus and fractional-variational problems with compositional functionals. Next, a review is made about the working mechanism of the Cuckoo search optimizer. After that, a simulation study is presented to discuss the differences between constant current and constant voltage charging methods in the case of fractional-order circuits. Following these, the optimization problem formulation used to get the approximate solutions of the optimal charging problem is presented. A summary of the optimization results is discussed and the concluding remarks are summarized.

Preliminaries

Definitions of fractional calculus are numerous and ever-increasing. So, recently, a classification was introduced in [63] and it categorized the fractional calculus operators into four main classes: Classical operators ($F1$), Modified operators ($F2$), Local operators ($F3$) and operators with non-singular kernel ($F4$). Riemann–Liouville and Caputo operators are example of the $F1$ class. They are defined as:

$$ {}^{RL}_{a}D^{\alpha}_{t}f(t) = \frac{1}{\Gamma(n-\alpha)} D^{n} \int_{a}^{t} (t-\tau)^{n-\alpha-1} f(\tau) d\tau, \tag{1a} $$

$$ {}^{C}_{a}D^{\alpha}_{t}f(t) = \frac{1}{\Gamma(n-\alpha)} \int_{a}^{t} (t-\tau)^{n-\alpha-1} f^{(n)}(\tau) d\tau, \tag{1b} $$

where $n-1 < v \leqslant n$ and $n \in \mathbb{N}$. The symbols ${}^{RL}_{a}D^{\alpha}_{t}$ and ${}^{C}_{a}D^{\alpha}_{t}$ refer to the fractional order Riemann–Liouville (RL) and Caputo derivative, respectively. The different succession of the fractional-order integral and integer order derivative observed in the definitions of RL and Caputo operators has affected their Laplace transform as follows:

$$\mathscr{L}\left\{{}^{RL}_{0}D^{\alpha}_{t}f(t)\right\} = s^{\alpha}F(s) - \sum_{k=0}^{n-1} s^{k}\left[{}_{0}D_{t}^{\alpha-k-1}f(t)\right]_{t=0}, \tag{2a}$$

$$\mathscr{L}\left\{{}^{C}_{0}D^{\alpha}_{t}f(t)\right\} = s^{\alpha}F(s) - \sum_{k=0}^{n-1} s^{\alpha-k-1}D^{k}f(0). \tag{2b}$$

Both definitions are equivalent under zero initial conditions. For linear fractional order circuits, the use of Laplace transform simplifies the analysis and saves the designer from the tedious time-domain expressions.

The calculus of variations approach for minimizing the energy loss inside the resistor in an integer order series *RC* circuit is formulated as [58]:

$$J = \int_{0}^{t_c} R_s C^2 \dot{v}_c{}^2(t)dt, \tag{3}$$

where t_c is the pre-specified charging time. The boundary conditions are

$$v_c(0) = 0, \quad v_c(t_c) = v_{max}, \tag{4}$$

where v_{max} is a design parameter, constrained by the device physics. There are two main approaches for solving calculus of variations problems. The *indirect* approach is the group of methods aiming at finding the extremal function through solving the associated Euler–Lagrange equation [58,64]. The *direct* approach is when the problem is tackled directly by optimizing the functional J and the resulting solutions do not have to satisfy the associated Euler–Lagrange equation as they are, in general, an approximate estimate of the extremal function [64]. The approach followed in [58] is of the indirect type and the paper studied three *RC* networks, the integer equivalent of the ones shown in Fig. 1, and their *RL* network duals.

In this work, the functional objective function takes the form:

$$J = \frac{C_{\alpha}\int_{0}^{t_c} v_c(t) \times D^{\alpha}v_c(t)dt}{\int_{0}^{t_c} v_{in}(t) \times i_{in}(t)dt}, \tag{5}$$

which is the ratio between the energy delivered to the fractional capacitor to the energy drawn from the source (charging efficiency). It is worth mentioning that $i_{in}(t)$ is a function of $v_c(t)$ and its fractional derivative for the three circuits under study (see Fig. 1). Such functionals are called composition functionals and the discussions on methods of their solutions in integer and fractional calculus of variation literature are very rare [65,66]. The only paper discussing a form of this fractional calculus of variations with composition functional is [65], where the authors adopted the indirect approach by deriving the associated Euler–Lagrange equation. The composition functional involved functional (fractional integration) and fractional derivative of Jumarie type of the same fractional-order and it is known that the satisfaction of the Euler–Lagrange equation is a necessary but not sufficient condition for optimality. Also, the resultant Euler–Lagrange equations in fractional calculus of variations are known to contains both left and right fractional derivative which is still a new topic in fractional differential equations theory [67]. These reasons make the only approach in literature [65], not suitable for our problem. So, We are motivated to use the direct method of optimization with Cuckoo search optimizer. The details of the optimization algorithm and the fractional calculus of variations problem formulation is discussed in the next two sections.

Cuckoo optimization

Cuckoo search optimization is inspired by the egg-laying and parasitic behavior of the Cuckoo bird [68,69]. The adult birds lay their eggs in other birds nests. They choose nests where the host bird just laid its eggs. The eggs grow and mature if not discovered by the host bird, and in general, they hatch earlier than the host bird eggs and the host bird indistinctly blindly propels the other unhatched eggs, which improve the food share of the parasitic cuckoo chicks [69,52]. Some female cuckoo birds can reproduce eggs that are indistinguishable from the colors and patterns of some host species reducing their chances of being discovered and increasing their survival rates [52]. The optimization algorithm follows three main hypotheses [53]. The first is that each adult bird lays only one egg each time. The second is that the adult Cuckoo bird puts its eggs in randomly chosen nest and the best found nest is saved for the next generation. The last hypothesis is that the host bird can discover the strange egg with a probability $p_a \in [0, 1]$.

It is known that animals search for food follows a random or at least a quasi-random pattern in nature. The foraging path can be seen as a random walk as it is affected by the current location and the transition probabilities to neighboring locations. For Cuckoo, and many birds and insects, this random walk has characteristics of a Lévy flight where the step sizes are evaluated according to a heavy-tailed probability distribution.

The mathematical formulation of the Cuckoo search algorithm is as follows. The location update of the global random walk equation is [70]:

$$Z_i^{t+1} = Z_i^t + \alpha \times Levy(s, \lambda), \tag{6}$$

where α is the step size scaling factor which is related to the scale of the problem under investigation. α is usually set to $1, L/10$, or $L/100$, where L is the scale of the problem [71,70]. s is the step size and the Levy flight is calculated by

$$L(s, \lambda) = \frac{\lambda\Gamma(\lambda)\sin(\pi\lambda/2)}{\pi s^{1+\lambda}}, \quad (s \gg s_0 > 0). \tag{7}$$

The local random walk is defined as [70]:

$$Z_i^{t+1} = Z_i^t + \alpha s \otimes H(p_a - \epsilon) \otimes \left(Z_j^t - Z_k^t\right), \tag{8}$$

where $H()$ is the Heaviside function, ϵ is a uniformly distributed random variable, p_a is the switching parameter, and Z_j and Z_k are

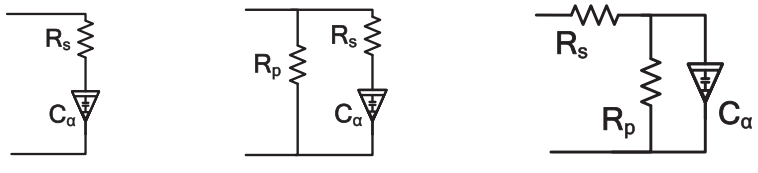

(a) (b) (c)

Fig. 1. The three supercapacitor equivalent circuit models under investigation: (a) R_s-CPE model (Model 1), (b) R_p-R_s-CPE model (Model 2), and (c) R_s-R_p-CPE model (Model 3).

two randomly selected solutions. The symbol $\otimes$ means element wise vector multiplication.

A comparison among basic charging methods

In this section, a numerical comparison is made between constant current, CC, and constant voltage, CV, charging methods in case of fractional-order series *RC* circuit.

First, for CV charging, the time needed to reach from 0% to 98% of the final voltage is calculated by [72]:

$$-zE_{\alpha,\alpha+1}(z) - 0.98 = 0, \quad z$$

where $E_{\alpha,\beta}(z)$ is the two parameter Mittag–Leffler (ML) function defined as [73]:

$$E_{\alpha,\beta}(z) = \sum_{k=0}^{\infty} \frac{z^k}{\Gamma(\alpha k + \beta)}. \tag{10}$$

Fig. 2(a) shows the numerical solution of this equation for $R_s = 10, C_\alpha \in \left[10^{-12}, 10^{0}\right] F \cdot sec^{\alpha-1}$ and $\alpha \in (0.5, 1.0]$. The roots where calculated using MATLAB *fzero* function using the ML implementation provided in [74]. When considering the change with respect to α, the behaviour of the CV charging time changes from increasing by increasing α at $C_\alpha = 10^{-12}$ to decreasing by increasing α at $C_\alpha = 1$. However, at constant α, the charging time increases by increasing C_α, as expected. At the end of this CV charging time, the final delivered electric charge can be calculated from [75]:

$$Q_{final,CV} = \frac{V_{max}}{R_s} t\, E_{\alpha,2}\left(-\frac{t^\alpha}{R_s C_\alpha}\right), \tag{11}$$

where V_{max} is the final voltage of the CPE which is equal to the constant voltage source. The current passing through the resistor during CV charging is given by [75]:

$$i_{R_s}(t) = \frac{V_{max}}{R_s} E_{\alpha,1}\left(-\frac{t^\alpha}{R_s C_\alpha}\right). \tag{12}$$

Hence, the energy dissipation in the resistor is calculated by:

$$E_{loss,CV} = R_s \int_0^{t_{CV}} (i_{R_s}(t))^2 dt. \tag{13}$$

Based on numerical simulation, the absolute difference between the lost energy at $\alpha = 0.5$ and $\alpha = 1$ is smaller for larger values of C_α. This means that the larger the capacitance is, the less effective α becomes in determining the energy loss. From MATLAB numerical simulations, it can be inferred that the efficiency is not changing with C_α which might be counter-intuitive. However, it is worth noting that, the CV charging time is not constant in these simulations and is a function of α and C_α.

Suppose that CC charging is performed within the same CV charging time (t_{CV}) and reaching the same final voltage on the CPE (V_{max}), the corresponding delivered electric charge to the CPE is calculated as [76]:

$$Q_{final,CC} = \frac{V_{max} C_\alpha \Gamma(1+\alpha)}{t_{CV}^{\alpha-1}}. \tag{14}$$

The ratio between the electric charge delivered to the CPE of CC charging divided by CV charging, $Q_{final,CC}/Q_{final,CV}$, is shown in Fig. 2(b). It is noticed that $Q_{final,cc}$ is always smaller than $Q_{final,cv}$ for $\alpha < 0.97$ where $\alpha \approx 0.97$ is the point where both electric charges are equal and for $\alpha > 0.97$ an opposite behaviour is observed. The energy loss due to the resistive element in CC charging is:

$$E_{loss,CC} = R_s \int_0^{t_{CV}} \left(\frac{V_{max} C_\alpha \Gamma(1+\alpha)}{t_{CV}^{\alpha}}\right)^2 dt. \tag{15}$$

Fig. 2(c) shows the quotient of energy loss in case on CC and CV. It is noticed that the energy loss in CC is always smaller than CV. Consequently, Fig. 2(d) shows that the charging efficiency in case of CC is always greater than its equivalent CV.

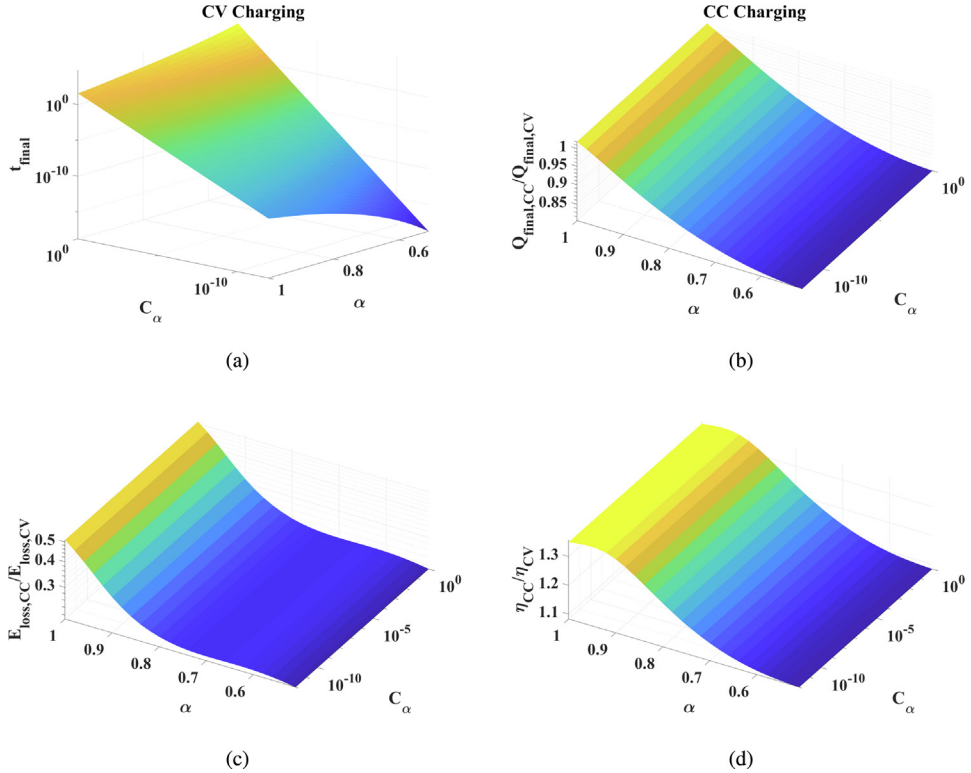

Fig. 2. The constant voltage and constant current charging techniques comparison at $R_s = 10$.

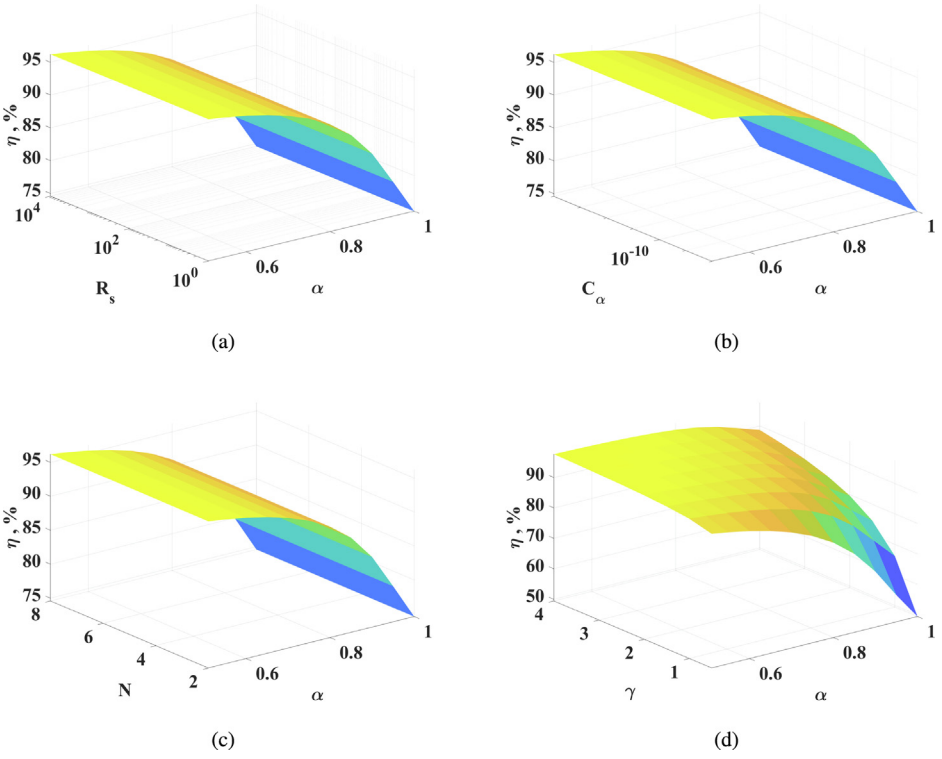

Fig. 3. R_s-CPE model maximum efficiency results.

Table 1
R_s-CPE model optimum charging voltage curves.

$R_s = 1\Omega$	$R_s = 10k\Omega$
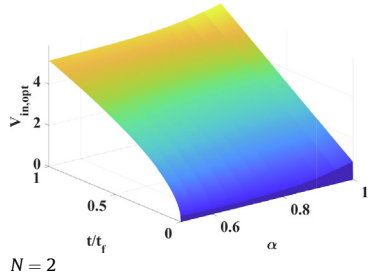	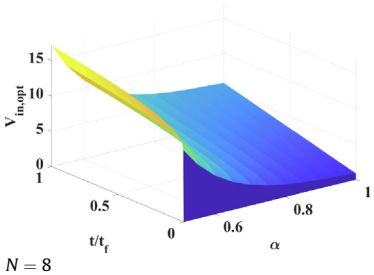
$N = 2$	$N = 8$
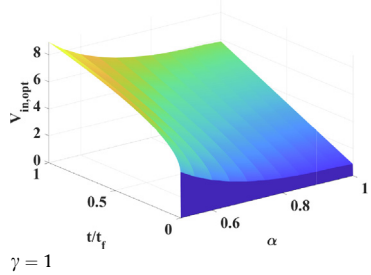	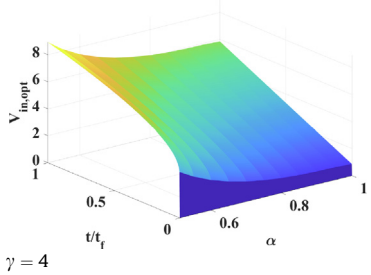
$\gamma = 1$	$\gamma = 4$
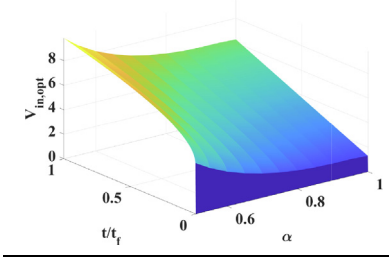	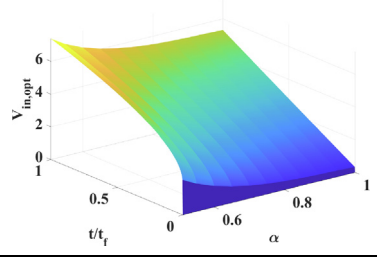

Optimization problem formulation

Assume the capacitor voltage is given as $v_c(t)$. The boundary conditions of the charging problem are:

$$v_c(0) = 0, \quad v_c(t_c) = v_{max}. \tag{16}$$

The charging time t_c is chosen to be a multiple of the 98% constant voltage charging time which is calculated as the root of Eq. (9). The charging time used in this work is defined as: $t_c = \gamma t_{CV}$ where γ is a tunable parameter used for numerical investigations.

The target is to maximize the charging efficiency defined by:

$$\eta_{charging} = \frac{E_C}{E_{in}}, \tag{17}$$

where E_C is the energy delivered to the capacitor, and E_{in} is the energy delivered by the source. The energy delivered to the CPE is calculated by:

$$E_{C\alpha} = C_\alpha \int_0^{t_c} v_c(t) D^\alpha v_c(t)\, dt. \tag{18}$$

and the input energy is given by:

$$E_{in} = \int_0^{t_c} v_{in} i_{in}\, dt. \tag{19}$$

Assume that the voltage across the fractional capacitor has the form:

$$v_c(t) = \sum_{i=1}^{N} a_i \left(\frac{t}{t_c}\right)^{b_i}, \quad a_N = v_{max} - \sum_{i=1}^{N-1} a_i, \tag{20}$$

where N is the number of terms used for the approximation. The condition on the last coefficient a_N is made to make sure that the prototype CPE voltage function, Eq. (20), satisfies the boundary condition for any choice of the search parameters. The α-order fractional Caputo derivative of the CPE voltage is given as:

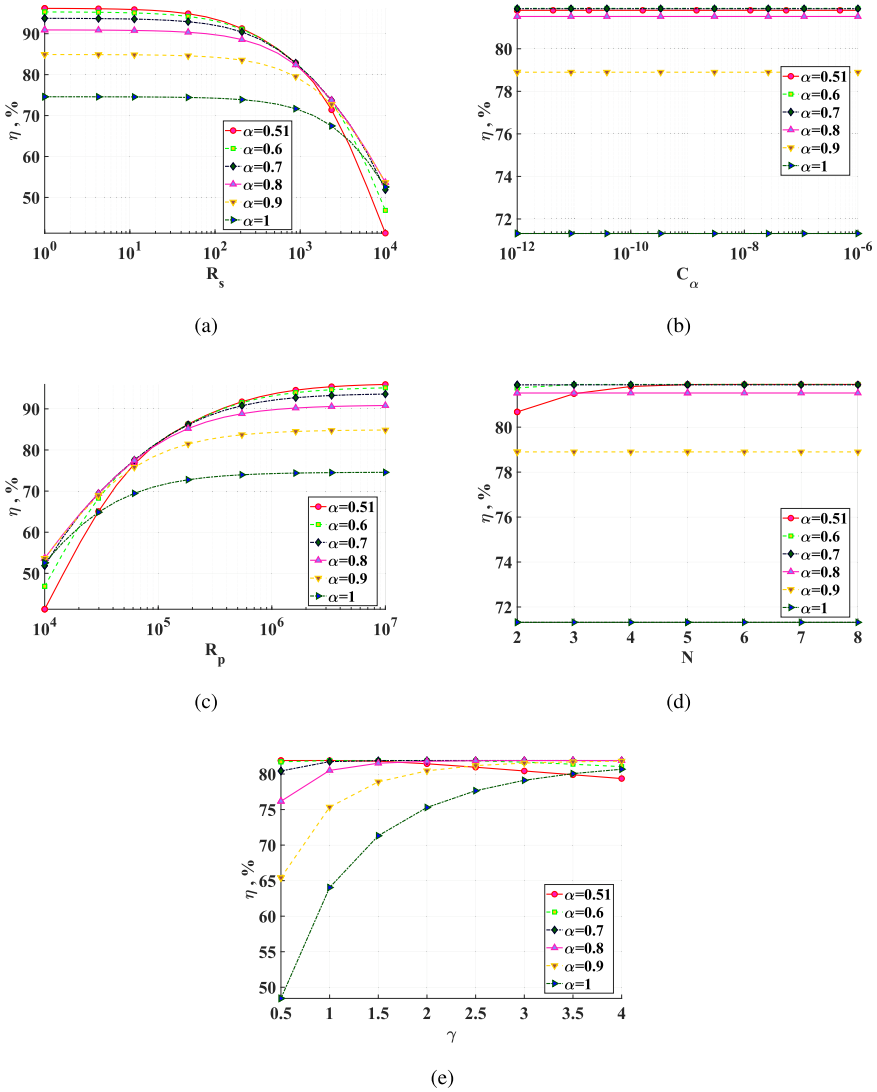

Fig. 4. R_p-R_s-CPE model maximum efficiency results.

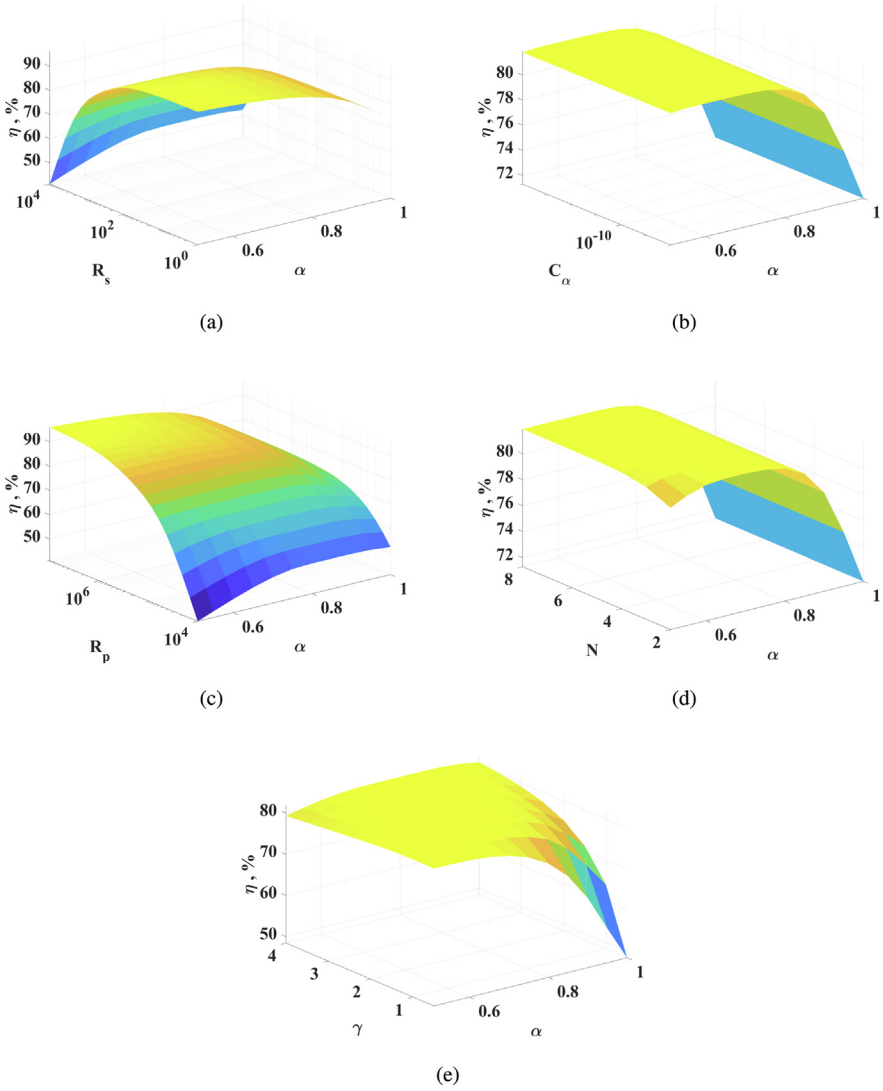

Fig. 5. R_s-R_p-CPE model maximum efficiency results.

$$D^{\alpha} v_c(t) = \sum_{i=1}^{N} \frac{a_i}{t_f^{b_i}} \frac{\Gamma(b_i+1)}{\Gamma(b_i-\alpha+1)} t^{b_i-\alpha}. \tag{21}$$

Hence, the search vector X is of length $2N-1$ is defined as: $X = [a_1, a_2, \ldots, a_{N-1}, b_1, b_2, \ldots, b_N]$. Throughout this work, the lower and upper bounds of the search space are given as: $Lb = \left[\underbrace{0, 0, \ldots, 0}_{N-1}, \underbrace{\alpha, \alpha, \ldots, \alpha}_{N}\right]$, and $Ub = \left[\underbrace{v_{max}, v_{max}, \ldots, v_{max}}_{N-1}, \underbrace{2N, 2N, \ldots, 2N}_{N}\right]$. The second section of the lower bound is set to α to avoid infinite current at $t = 0$. The number of search agents is $7 \times (2N-1)$ and the number of iterations is 1000. For each set of parameters, ten independent runs are executed and only the best run is chosen.

The input voltage in case of the R_s-CPE model:

$$v_{in} = v_c(t) + R_s C_{\alpha} D^{\alpha} v_c(t), \tag{22}$$

while the input current is:

$$i_{in} = C_{\alpha} D^{\alpha} v_c(t). \tag{23}$$

The input voltage in case of R_p-R_s-CPE model:

$$v_{in} = v_c(t) + R_s C_{\alpha} D^{\alpha} v_c(t), \tag{24}$$

while the input current in this case is

$$i_{in} = \frac{v_{in}}{R_p} + C_{\alpha} D^{\alpha} v_c(t). \tag{25}$$

The input current in case of the R_s-R_p-CPE model:

$$i_{in} = \frac{v_c(t)}{R_p} + C_{\alpha} D^{\alpha} v_c(t), \tag{26}$$

while the input voltage:

$$v_{in} = v_c(t) + i_{in} \times R_s. \tag{27}$$

Table 2
R_p-R_s-*CPE* model optimum charging voltage curves.

$R_s = 1\Omega$	$R_s = 10k\Omega$
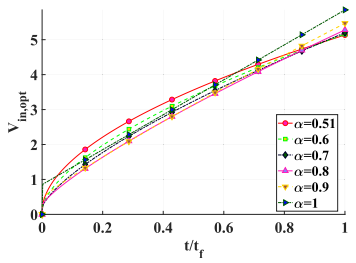	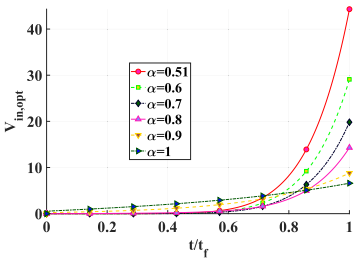
$R_p = 10k\Omega$	$R_p = 10M\Omega$
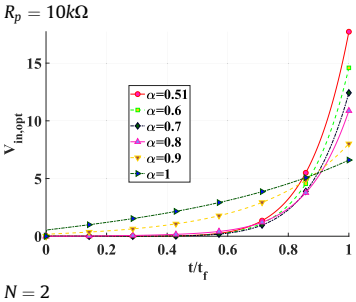	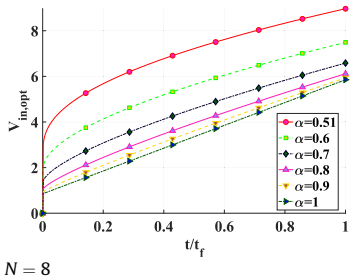
$N = 2$	$N = 8$
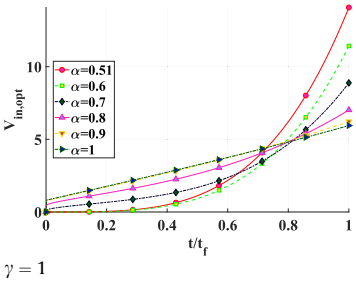	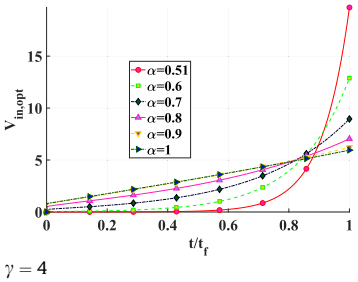
$\gamma = 1$	$\gamma = 4$
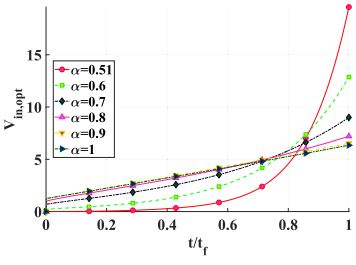	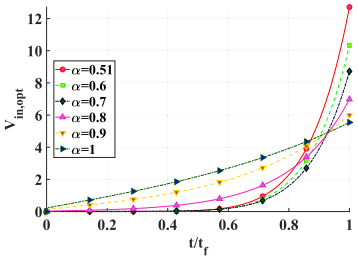

Table 3
R_s-R_ps-*CPE* model optimum charging voltage curves.

$R_s = 1\Omega$	$R_s = 10k\Omega$
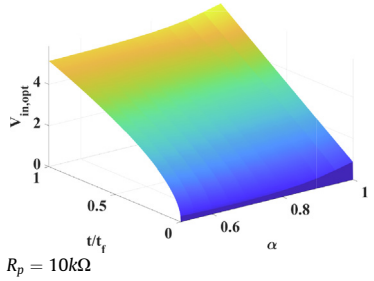	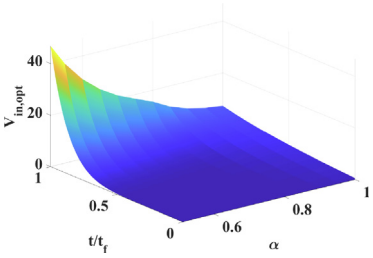
$R_p = 10k\Omega$	$R_s = 10M\Omega$
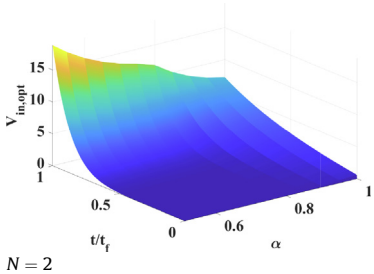	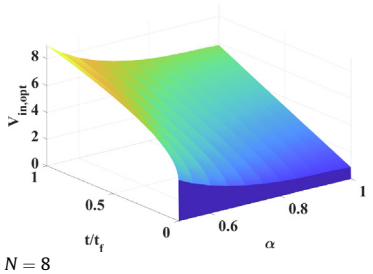
$N = 2$	$N = 8$
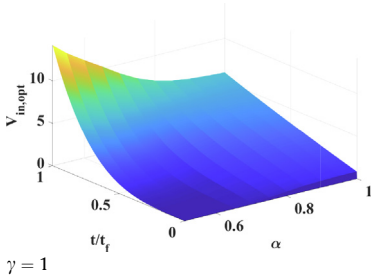	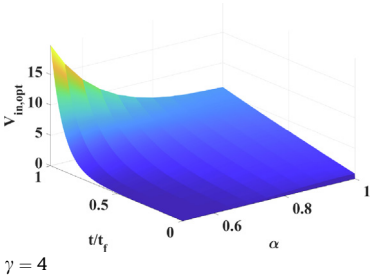
$\gamma = 1$	$\gamma = 4$
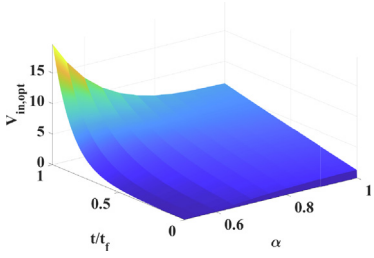	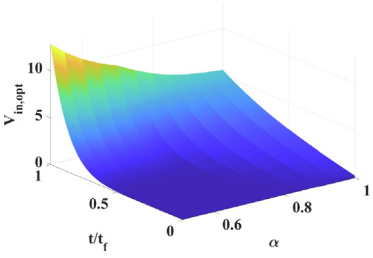

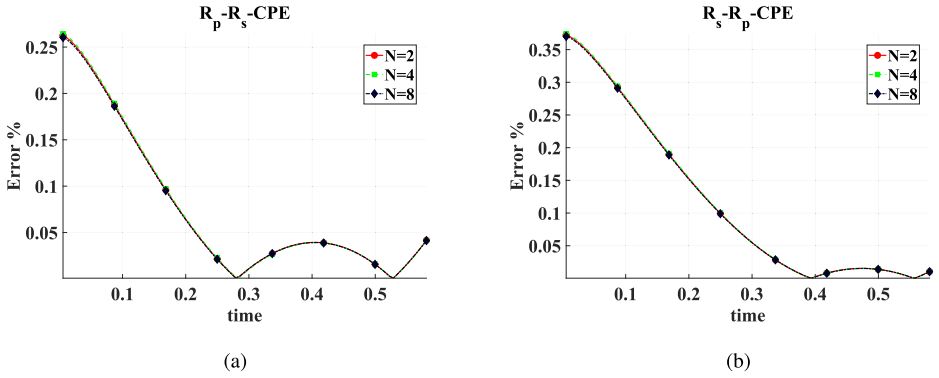

Fig. 6. Percentage error of the optimal v_{in} of this work and the analytical expression of [58].

Results and discussion

Algorithm 1. steps for simulation study

1: Input: circuit number; 1 for R_s-*CPE*, 2 for R_p-R_s-*CPE*, or 3 for R_s-R_p-*CPE*
2: Set parameter sweep ranges
3: $R_s = 10^0 : 10^4$, 20 log-spaced points.
4: $C_\alpha = 10^{-12} : 10^{-6}$, 20 log-spaced points.
5: $R_p = 10^4 : 10^7$, 20 log-spaced points.
6: $N = 2 : 8$ with 1 step.
7: $\gamma = 0.5 : 4$ with 0.5 step.
8: $\alpha = 0.51 : 1.0$ with 0.05 step.
9: **for all** Sweep Parameters **do**
10: **for all** α **do**
11: Set parameters to default values
12: $R_s = 1k, C_\alpha = 100p, R_p = 100k, \gamma = 1.5, V_{max} = 5, N = 4$.
13: Change the default value for the parameter being swept.
14: Calculate t_{CV} from Eq. (9) then multiply it by γ to get t_c.
15: Run Cuckoo search 10 times using the objective function of Eq. (17) and the lower and upper boundaries discussed before. Save the optimal positions of Eq. (20).
16: **end for**
17: **end for**

In this section, the optimization results are discussed for the three circuit under investigation: R_s-*CPE*, R_p-R_s-*CPE*, and R_s-R_p-*CPE* and a brief of the simulation procedure is summarized in Algorithm 1. The default parameters are: $R_s = 1k, C_\alpha = 100p, R_p = 100k, \gamma = 1.5$, and $N = 4$. These parameters are guided from the study made in [58]. Each objective function evaluation is made with a time vector of length $numPoints = 500$ for good accuracy and $v_{max} = 5V$. The choice of V_{max} is only constrained by the device physics and does not affect the results due to the linearity of the problem. Five different sweep planes are studied for each circuit except the R_s-*CPE* case has only four as it doesn't include the R_p parameter. The two dimensional sweep planes are: α-R_s, α-C_α, α-R_p, α-N, and α-γ. The ranges of the parameters are: $\alpha \in [0.51, 1]$ with a step of 0.05, $R_s \in \left[10^0, 10^4\right]\Omega$ logarithmically spaced vector of length 20, $C_\alpha \in \left[10^{-12}, 10^{-6}\right]$ $F \cdot sec^{\alpha-1}$ logarithmically spaced vector of length 20, $R_p \in \left[10^4, 10^7\right]\Omega$ logarithmically spaced vector of length 20, $N \in [2, 8]$ with a step of 1, and $\gamma \in [0.5, 4]$ with a step of 0.5. The range of α has been chosen in accordance with the estimated parameters obtained in recent literature via time or frequency domain data [30,75,77–79] Each optimization made in the study space is performed ten times and the best solution in terms of objective function is chosen to be included in all the different plots/tables presented. For each circuit, efficiency surfaces over the study planes and sample charging curves are provided for discussion. The charging curves were chosen for the following parameter values: $R_s = 1\Omega, R_s = 10k\Omega, R_p = 10k\Omega, R_p = 10M\Omega$, $N = 2, N = 8, \gamma = 1$, and $\gamma = 4$ and simulated against a normalized time axis due to the discrepancy of charging times at different values of α and the sweep parameter.

The maximum efficiency results for the R_s-*CPE* circuit are shown in Fig. 3. The charging efficiency decreases with increasing α, which is in accordance with the analysis in [62]. However, as mentioned in [62], the round trip efficiency decreases by increasing α due to the leaky behaviour of the CPE. For the sweep parameters R_s and C_α, the maximum efficiency seems to be independent of them. This is expected as the charging time is evaluated according to Eq. (9) and it is dependent on both R_s and C_α. So, there is a compensation between their values and the charging time to achieve nearly constant efficiency at the same α. For the N parameter, it is observed that the maximum efficiency is independent of this parameter too. This is observed from the numerical results of the optimal coefficients of Eq. (20) for this case. The coefficients, a_k, are zeros except for the first one and the corresponding power, b_1, is approximately equal to α which means that the constant current input is the most efficient method to charge the R_s-*CPE* circuit confirming the analytical study in [62]. For the last parameter, γ, the charging efficiency increases by increasing γ as we know from the integer case. However, the gap between the charging efficiencies at $\gamma = 0.5$ and $\gamma = 4$ is very small at $\alpha = 0.51$ and gradually increases until it reaches the maximum value at $\alpha = 1$. A sample of optimal charging curves for the R_s-*CPE* case is shown in Table 1. As mentioned earlier, the optimal charging curves is found to be the constant current. Hence, the charging curves are all raised fractional power ramps of the form: $V_{in} = C_1 + C_2 t^\alpha$. Comparing the cases at $R_s = 1$ and $R_s = 10k\Omega$, the DC offset increases by increasing α for the first case and it does the opposite in the second case. Also, The final input voltage is larger by increasing α in the first case but is it gets smaller by increasing α in the second case. Overall, the final input voltage is much higher than the target CPE voltage for α near 0.5 and bigger R_s. For the N parameter, the optimal input voltage curves are identical in the cases $N = 2$ and $N = 8$ for the same reason mentioned above. Lastly, for the γ parameter, a higher value of DC offset and final input voltage is observed in case of $\gamma = 1$. This is expected as faster charging requires higher input

Table 4
Cuckoo search algorithm's convergence curves (dashed) and their mean curve (solid) for selected cases of the three fractional-order *RC* circuits under investigation.

R_s-*CPE*	$R_s = 4.28\Omega, \alpha = 0.9, CoV = 1.83 \times 10^{-12}$	$N = 5, \alpha = 0.85, CoV = 2.43 \times 10^{-10}$
R_p-R_s-*CPE*	$R_s = 78.47\Omega, \alpha = 0.95, CoV = 4.36 \times 10^{-10}$	$R_p = 2.34M\Omega, \alpha = 0.9, CoV = 8.26 \times 10^{-11}$
R_s-R_p-*CPE*	$R_p = 0.264M\Omega, \alpha = 0.95, CoV = 1.5 \times 10^{-9}$	$\gamma = 0.5, \alpha = 0.95, CoV = 1.02 \times 10^{-9}$

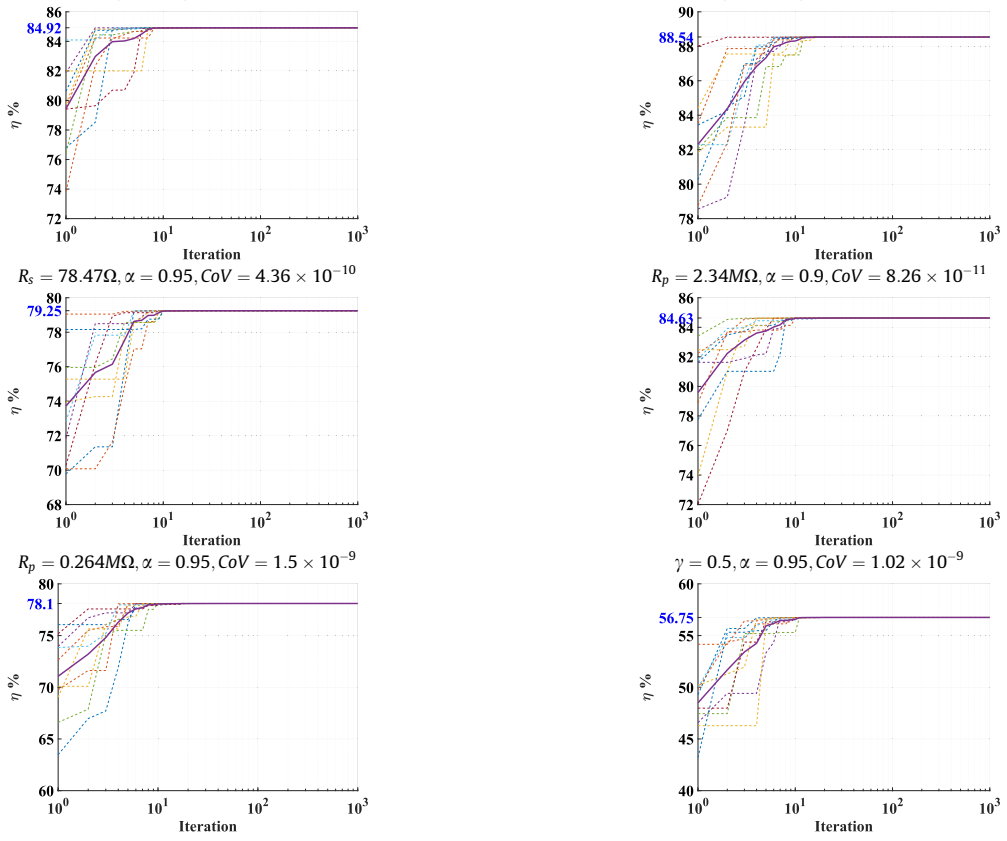

voltage which leads to higher current and consequently higher resistive losses.

The behaviors of the R_p-R_s-*CPE* and R_s-R_p-*CPE* circuits are similar when comparing them qualitatively. The efficiency surfaces are illustrated in Fig. 4 and Fig. 5. For the R_s parameter, a higher R_s means longer charging time t_c. However, in the presence of R_p at constant α, this leads to higher losses and efficiency degradation. For $R_s = 1\Omega$, the efficiency is higher for lower α and the opposite happens at $R_s = 10k\Omega$. For the R_p parameter at constant α, the efficiency increases by increasing R_p due to lower leakages. At $R_p = 10k\Omega$, the efficiency increases by increasing α and the opposite happens at $R_p = 10M\Omega$. The N parameter effect is present for low α only. It is evident that for $0.5 < \alpha < 0.6$, three to four terms of Eq. (20) are needed to obtain the maximum efficiency. On the other hand, at $\alpha > 0.6$, two terms are enough to obtain a reasonable approximation of the optimal charging input function. The γ parameter is obvious in the integer case $\alpha = 1$ as the efficiency is increased by increasing γ. However, this effect is negligible at $\alpha = 0.51$ where a slight decrease in efficiency is observed as γ increases.

The optimal input voltage charging curves are shown for selective cases in Tables 2 and 3. For $R_s = 1\Omega$ and $R_s = 10k\Omega$, The final input voltage value is increased by increasing R_s and decreasing α. The optimal input voltage curve is similar to the R_s-*CPE* case when R_s is negligible in comparison with R_p which is the case for the figure at $R_s = 1\Omega$ and the figure at $R_p = 10M\Omega$. The N parameter effect is shown in the optimal charging curves near $\alpha = 0.51$ and has no effect at $\alpha = 1$. For the last parameter, γ, increasing γ puts lower stress on the supply by requiring smaller voltage. However, lower values of α always requires higher final input voltage values at the same γ value. Another observation is the higher amount of change in the value of the input voltage is seen during the second half of the charging period, specially for low α values.

For validation with the integer case, the optimal input voltages as in [58] during the charging period:

$$v_{in,1}(t) = A_h\left[\frac{1}{\sigma}\cosh\frac{t}{\sigma\tau_1} + \sinh\frac{t}{\sigma\tau_1}\right] \tag{28a}$$

$$v_{in,2}(t) = \beta A_h\left[\frac{1}{\sigma}\cosh\frac{t}{\sigma\tau_2} + \sinh\frac{t}{\sigma\tau_2}\right] \tag{28b}$$

for the R_p-R_s-*CPE*, and R_s-R_p-*CPE* cases, respectively. Where:

$$\begin{aligned} A_h &= V_{max}csch\left(\tfrac{t_c}{\sigma\tau}\right),\ \tau_1 = R_sC,\ \tau_2 = \tfrac{R_sR_p}{R_s+R_p}C, \\ \sigma &= \sqrt{1+\tfrac{R_p}{R_s}},\ \beta = 1+\tfrac{R_s}{R_p} \end{aligned} \tag{29}$$

The percentage error between the optimal input voltage expressions in Eq. (28) derived in [58] and the optimal input voltages obtained using the Cuckoo search optimizer are shown in Fig. 6. It can be seen that the percentage error does not exceed 0.26% in case of R_p-R_s-*CPE* circuit and 0.37% in case of R_s-R_p-*CPE* model for the default parameters discussed in previous sections. This means that the result of our approach is identical to the one derived analytically in [58] at $\alpha = 1$.

In order to test the consistency and convergence speed of the utilized meta-heuristic optimizer, the convergence curves of 10 independent runs and their mean are shown for selected cases of the parameter space in Table 4. In all cases, the optimal efficiency is reached before 100 iterations of the optimizer and in some cases

it is reached as fast as 10 iterations only. Also, the coefficient of variation, $CoV = std/mean$, of the optimal efficiency reached is calculated for each case. It is below 2×10^{-9} in the selected cases which verifies the consistency of Cuckoo search optimizer in solving the investigated problem.

Conclusion

The optimal charging for three fractional-order *RC* circuits was investigated. The problem was formulated to find the optimal voltage charging curve that maximizes the charging efficiency, which is the energy delivered to the capacitor divided by the supply's energy. The cuckoo search optimizer was used to find optimal coefficients and powers of the capacitor voltage prototype function. The results were discussed for the fractional-order $0.5 < \alpha \leq 1.0$ and a wide range of circuit parameters, charging condition and approximation order like: C_α, R_s, R_p, t_f, and N. It was noticed that the resistive parameters and charging time t_f have the most dominant effect on the efficiency and the approximation order of 4, of the prototype capacitor voltage function, is enough in most cases. The same procedure can be applied to fractional-order *RL* circuits. In fact, fractional-order *RL* circuits can be considered as the dual problem of what we discussed, fractional-order *RC* circuits, where the optimal expressions for current and voltage are to be interchanged in order to get the optimal expressions for the other problem similar to what was done in [58]. Possible future work includes investigating the effect of different fractional-calculus definitions on this problem, optimal charging, similar to the analysis performed in [79,22,23].

Compliance with Ethics Requirements

This article does not contain any studies with human or animal subjects.

Declaration of Competing Interest

The authors declare that they have no known competing financial interests or personal relationships that could have appeared to influence the work reported in this paper.

References

[1] Failla G, Zingales M. Advanced materials modelling via fractional calculus: challenges and perspectives. Philos Trans Roy Soc A: Math Phys Eng Sci 2020;378(2172):20200050. ISSN 1364-503X.

[2] Khubalkar S, Junghare A, Aware M, Das S. Unique fractional calculus engineering laboratory for learning and research. Int J Electric Eng Edu 2020;57(1):3–23.

[3] Tarasov VE. Mathematical economics: application of fractional calculus. Mathematics 2020;8(5):660.

[4] Machado JAT, Kiryakova V. Recent history of the fractional calculus: data and statistics. Berlin, Boston: De Gruyter; 2019. p. 1–22.

[5] Malesza W, Macias M, Sierociuk D. Analytical solution of fractional variable order differential equations. J Comput Appl Math 2019;348:214–36. ISSN 0377-0427.

[6] Petráš I, Terpák J. Fractional calculus as a simple tool for modeling and analysis of long memory process in industry. Mathematics 2019;7(6):511.

[7] ElSafty AH, Tolba MF, Said LA, Madian AH, Radwan AG. A study of the nonlinear dynamics of human behavior and its digital hardware implementation. J Adv Res 2020; 25: 111–23, ISSN 2090–1232, recent Advances in the Fractional-Order Circuits and Systems: Theory, Design and Applications.

[8] Silva-Juárez A, Tlelo-Cuautle E, de la Fraga LG, Li R. FPAA-based implementation of fractional-order chaotic oscillators using first-order active filter blocks. J Adv Res 2020. ISSN 2090-1232.

[9] Ismail SM, Said LA, Rezk AA, Radwan AG, Madian AH, Abu-Elyazeed MF, et al. Generalized fractional logistic map encryption system based on FPGA. AEU – Int J Electron Commun 2017;80:114–26. ISSN 1434–8411..

[10] Ismail SM, Said LA, Radwan AG, Madian AH, Abu-ElYazeed MF. A novel image encryption system merging fractional-order edge detection and generalized chaotic maps. Signal Process 2020;167:107280. ISSN 0165-1684.

[11] Yao J, Wang K, Huang P, Chen L, Machado JT. Analysis and implementation of fractional-order chaotic system with standard components. J Adv Res 2020; 25: 97–109, ISSN 2090-1232, recent Advances in the Fractional-Order Circuits and Systems: Theory, Design and Applications.

[12] Tufenkci S, Senol B, Alagoz BB, Matušu R. Disturbance rejection FOPID controller design in v-domain. J Adv Res 2020, ISSN 2090-1232.

[13] Sweilam N, AL-Mekhlafi S, Baleanu D. A hybrid fractional optimal control for a novel Coronavirus (2019-nCov) mathematical model. J Adv Res 2020, ISSN 2090-1232.

[14] Birs I, Nascu I, Ionescu C, Muresan C. Event-based fractional order control. J Adv Res 2020; 25: 191–203, ISSN 2090–1232, recent Advances in the Fractional-Order Circuits and Systems: Theory, Design and Applications.

[15] Zhang Z. Fractional-order time-sharing-control-based wireless power supply for multiple appliances in intelligent building. J Adv Res 2020, ISSN 2090-1232.

[16] Shu X, Zhang B, Rong C, Jiang Y. Frequency bifurcation in a series-series compensated fractional-order inductive power transfer system. J Adv Res 2020;25:235–42. ISSN 2090-1232, recent Advances in the Fractional-Order Circuits and Systems: Theory, Design and Applications..

[17] Hosny KM, Darwish MM, Eltoukhy MM. New fractional-order shifted Gegenbauer moments for image analysis and recognition. J Adv Res 2020, ISSN 2090-1232.

[18] Soltan A, Radwan AG, Soliman AM. Fractional-order mutual inductance: analysis and design. Int J Circuit Theory Appl 2016;44(1):85–97.

[19] Tenreiro Machado J, Lopes AM. Multidimensional scaling locus of memristor and fractional order elements. J Adv Res 2020; 25: 147–57, ISSN 2090-1232, recent Advances in the Fractional-Order Circuits and Systems: Theory, Design and Applications.

[20] Jiang Y, Zhang B, Shu X, Wei Z. Fractional-order autonomous circuits with order larger than one. J Adv Res 2020; 25: 217–25, ISSN 2090-1232, recent Advances in the Fractional-Order Circuits and Systems: Theory, Design and Applications.

[21] Gómez-Aguilar JF, Dumitru B. Fractional transmission line with losses. Zeitschrift für Naturforschung A 2014;69(10–11):539–46.

[22] Gómez-Aguilar JF, Atangana A, Morales-Delgado VF. Electrical circuits RC, LC, and RL described by Atangana-Baleanu fractional derivatives. Int J Circuit Theory Appl 2017;45(11):1514–33.

[23] Gómez-Aguilar J, Morales-Delgado V, Taneco-Hernández M, Baleanu D, Escobar-Jiménez R, Qurashi MA. Analytical solutions of the electrical RLC circuit via Liouville-Caputo operators with local and non-local kernels. Entropy 2016;18(8):402.

[24] Morales-Delgado VF, Gómez-Aguilar JF, Taneco-Hernández MA, Escobar-Jiménez RF. Fractional operator without singular kernel: applications to linear electrical circuits. Int J Circuit Theory Appl 2018;46(12):2394–419.

[25] Aguilar JFG. Behavior characteristics of a cap-resistor, memcapacitor, and a memristor from the response obtained of RC and RL electrical circuits described by fractional differential equations. Turk J Electric Eng Comput Sci 2016;24:1421–33.

[26] Gómez-Aguilar J, Yépez-Martínez H, Escobar-Jiménez R, Astorga-Zaragoza C, Reyes-Reyes J. Analytical and numerical solutions of electrical circuits described by fractional derivatives. Appl Math Modell 2016; 40 (21): 9079–94, ISSN 0307-904X.

[27] Said LA, Radwan AG, Madian AH, Soliman AM. Three fractional-order-capacitors-based oscillators with controllable phase and frequency. J Circ Syst Comput 2017;26(10):1750160.

[28] Elwy O, Rashad SH, Said LA, Radwan AG. Comparison between three approximation methods on oscillator circuits. Microelectron J 2018; 81: 162–78, ISSN 0026-2692.

[29] Yu M, Li Y, Podlubny I, Gong F, Sun Y, Zhang Q, Shang Y, et al. Fractional-order modeling of lithium-ion batteries using additive noise assisted modeling and correlative information criterion. J Adv Res 2020, ISSN 2090-1232.

[30] Allagui A, Freeborn TJ, Elwakil AS, Fouda ME, Maundy BJ, Radwan AG, et al. Review of fractional-order electrical characterization of supercapacitors. J Power Sources 2018;400:457–67. ISSN 0378-7753.

[31] Hidalgo-Reyes J, Gómez-Aguilar J, Escobar-Jiménez R, Alvarado-Martínez V, López-López M. Classical and fractional-order modeling of equivalent electrical circuits for supercapacitors and batteries, energy management strategies for hybrid systems and methods for the state of charge estimation: a state of the art review. Microelectron J 2019; 85: 109–28, ISSN 0026-2692.

[32] Fu B, Freeborn TJ. Cole-impedance parameters representing biceps tissue bioimpedance in healthy adults and their alterations following eccentric exercise. J Adv Res 2020, ISSN 2090-1232.

[33] Yousri D, AbdelAty AM, Said LA, AboBakr A, Radwan AG. Biological inspired optimization algorithms for cole-impedance parameters identification. AEU – Int J Electron Commun 2017;78:79–89. ISSN 1434-8411.

[34] Tolba MF, Said LA, Madian AH, Radwan AG. FPGA implementation of the fractional order integrator/differentiator: two approaches and applications. IEEE Trans Circuits Syst I Regul Pap 2019;66(4):1484–95.

[35] Ortigueira MD, Bengochea G. Non-commensurate fractional linear systems: new results. J Adv Res 2020; 25: 11–7, ISSN 2090-1232, recent Advances in the Fractional-Order Circuits and Systems: Theory, Design and Applications.

[36] Aguilar JG, Baleanu D. Solutions of the telegraph equations using a fractional calculus approach. Proc Romanian Acad A 2014;15:27–34.
[37] Yang X-S. Nature-inspired optimization algorithms. Elsevier; 2014.
[38] Wolpert DH, Macready WG. No free lunch theorems for optimization. IEEE Trans Evol Comput 1997;1(1):67–82.
[39] Gholami-Boroujeny S, Bolic M. Extraction of Cole parameters from the electrical bioimpedance spectrum using stochastic optimization algorithms. Med Biol Eng Comput 2016;54(4):643–51.
[40] Yang Y, Ni W, Sun Q, Wen H, Teng Z. Improved Cole parameter extraction based on the least absolute deviation method. Physiol Meas 2013;34 (10):1239.
[41] Matos C, Ortigueira MD. Fractional filters: an optimization approach. In: Doctoral conference on computing, electrical and industrial systems, Springer; 2010. p. 361–6.
[42] Mahata S, Saha SK, Kar R, Mandal D. Optimal design of fractional-order digital differentiator using flower pollination algorithm. J Circ Syst Comput 2018;27 (08):1850129.
[43] Mahata S, Saha SK, Kar R, Mandal D. A metaheuristic optimization approach to discretize the fractional order Laplacian operator without employing a discretization operator. Swarm Evol Comput 2019; 44: 534–45, ISSN 2210-6502.
[44] Mahata S, Kar R, Mandal D. Optimal fractional-order highpass Butterworth magnitude characteristics realization using current-mode filter. AEU – Int J Electron Commun 2019; 102: 78–89, ISSN 1434-8411.
[45] Mahata S, Banerjee S, Kar R, Mandal D. Revisiting the use of squared magnitude function for the optimal approximation of (1+α)-order Butterworth filter. AEU – Int J Electron Commun 2019;110:152826. ISSN 1434-8411.
[46] Mahata S, Kar R, Mandal D. Comparative study of nature-inspired algorithms to design (1+α) and (2+α)-order filters using a frequency-domain approach. Swarm Evol Comput 2020; 55: 100685, ISSN 2210-6502.
[47] Mahata S, Kar R, Mandal D. Optimal rational approximation of bandpass Butterworth filter with symmetric fractional-order roll-off. AEU – Int J Electron Commun 2020; 117: 153106, ISSN 1434-8411.
[48] Soni A, Sreejeth N, Saxena V, Gupta M. Series optimized fractional order low pass butterworth filter. Arab J Sci Eng 2020;45(3):1733–47.
[49] Soni A, Gupta M. Analysis and design of optimized fractional order low pass bessel filter. J Circuits Syst Comput 2020 (ja).
[50] Soni A, Gupta M. Performance evaluation of different order fractional Chebyshev filter using optimisation techniques. Int J Electron Lett 2020;8 (2):205–22.
[51] Yousri D, AbdelAty AM, Radwan AG, Elwakil A, Psychalinos C. Comprehensive comparison based on meta-heuristic algorithms for approximation of the fractional-order Laplacian s^{α} as a weighted sum of first-order high-pass filters. Microelectron J 2019; 87: 110–20, ISSN 0026-2692.
[52] Joshi A, Kulkarni O, Kakandikar G, Nandedkar V. Cuckoo search optimization – a review. Mater Today: Proc 2017; 4(8): 7262-9, ISSN 2214-7853, international Conference on Advancements in Aeromechanical Materials for Manufacturing (ICAAMM-2016): Organized by MLR Institute of Technology, Hyderabad, Telangana, India.
[53] Yousri D, Mirjalili S. Fractional-order cuckoo search algorithm for parameter identification of the fractional-order chaotic, chaotic with noise and hyper-chaotic financial systems. Eng Appl Artif Intell 2020; 92: 103662, ISSN 0952-1976.
[54] Zou C, Zhang L, Hu X, Wang Z, Wik T, Pecht M. A review of fractional-order techniques applied to lithium-ion batteries, lead-acid batteries, and supercapacitors. J Power Sources 2018;390:286–96. ISSN 0378-7753.
[55] Wang Y, Chen Y, Liao X. State-of-art survey of fractional order modeling and estimation methods for lithium-ion batteries. Fract Calculus Appl Anal 2019;22(6):1449–79.
[56] Li H, Peng J, Zhou Y, He J, Huang Z, He L, et al. SoH-Aware charging of supercapacitors with energy efficiency maximization. IEEE Trans Energy Convers 2018;33(4):1766–75.
[57] Paul S, Schlaffer AM, Nossek JA. Optimal charging of capacitors. IEEE Trans Circuits Syst I: Fundamental Theory Appl 2000; 47(7): 1009–16, ISSN 1558-1268.
[58] Smunyahirun R, Tan EL. Derivation of the most energy-efficient source functions by using calculus of variations. IEEE Trans Circuits Syst I Regul Pap 2016;63(4):494–502.
[59] Smunyahirun R, Tan EL. Most energy-efficient input voltage function for RC delay line, in. In: 2018 IEEE international symposium on electromagnetic compatibility and 2018 IEEE Asia-Pacific symposium on electromagnetic compatibility. p. 1022–6.
[60] Parvini Y, Vahidi A. Optimal charging of ultracapacitors during regenerative braking. In: 2012 IEEE international electric vehicle conference 2012, p. 1–6, ISSN null.
[61] Smunyahirun R, Tan EL. Optimum lowest input energy for first-order circuits in transient state. In: 2017 14th international conference on Electrical Engineering/Electronics, Computer, Telecommunications and Information Technology (ECTI-CON), ISSN null; 2017, p. 143–6.
[62] AbdelAty A, Fouda ME, Elbarawy MT, Radwan A. Optimal charging and discharging of supercapacitors. J Electrochem Soc 2020;167(11):110521.
[63] Teodoro GS, Machado JT, de Oliveira EC. A review of definitions of fractional derivatives and other operators. J Comput Phys 2019; 388: 195–208, ISSN 0021-9991.
[64] Komzsik L. Applied calculus of variations for engineers. CRC Press; 2019.
[65] Malinowska AB, Ammi MRS, Torres DF. Composition functionals in fractional calculus of variations. Commun Fract Calculus 2010;1:32–40.
[66] Castillo E, Luceno A, Pedregal P. Composition functionals in calculus of variations: application to products and quotients. Math Models Meth Appl Sci 2008;18(01):47–75.
[67] Agrawal O. Formulation of Euler-Lagrange equations for fractional variational problems. J Math Anal Appl 2002; 272 (1): 368–79, ISSN 0022-247X.
[68] Yang X, Deb Suash. Cuckoo Search via Lévy flights. In: 2009 World Congress on Nature Biologically Inspired Computing (NaBIC); 2009, p. 210–4.
[69] Gandomi AH, Yang X-S, Alavi AH. Cuckoo search algorithm: a metaheuristic approach to solve structural optimization problems. Eng Comput 2013;29 (1):17–35.
[70] Yang X-S. Chapter 9 – Cuckoo Search. In: Yang X-S, editor, Nature-Inspired Optimization Algorithms, Elsevier, Oxford, 2014, ISBN 978-0-12-416743-8, p. 129–39.
[71] Kaveh A. Cuckoo search optimization. In: Advances in metaheuristic algorithms for optimal design of structures. Springer International Publishing; 2016. p. 321–52.
[72] AbdelAty AM, Radwan AG, Ahmed WA, Faied M. Charging and discharging RC_αcircuit under Riemann-Liouville and Caputo fractional derivatives. In: 2016 13th International Conference on Electrical Engineering/Electronics, Computer, Telecommunications and Information Technology (ECTI-CON); 2016, p. 1–4.
[73] Kilbas AA, Srivastava HM, Trujillo JJ. Theory and applications of fractional differential equations. vol. 204, Elsevier; 2006.
[74] Garrappa R. Numerical evaluation of two and three parameter Mittag-Leffler functions. SIAM J Numer Anal 2015;53(3):1350–69.
[75] Fouda ME, Elwakil AS, Allagui A. Commercial supercapacitor parameter estimation from step voltage excitation. Int J Circuit Theory Appl 2019;47 (10):1705–12.
[76] Allagui A, Freeborn TJ, Elwakil AS, Maundy BJ. Reevaluation of performance of electric double-layer capacitors from constant-current charge/discharge and cyclic voltammetry. Sci Rep 2016;6(1):1–8.
[77] Fouda ME, Allagui A, Elwakil AS, Eltawil A, Kurdahi F. Supercapacitor discharge under constant resistance, constant current and constant power loads. J Power Sources 2019; 435: 226829, ISSN 0378-7753.
[78] Krishnan G, Das S, Agarwal V. An online identification algorithm to determine the parameters of the fractional-order model of a supercapacitor. IEEE Trans Ind Appl 2020;56(1):763–70.
[79] Hidalgo-Reyes J, Gómez-Aguilar J, Escobar-Jimenez R, Alvarado-Martinez V, Lopez-Lopez M. Determination of supercapacitor parameters based on fractional differential equations. Int J Circuit Theory Appl 2019;47(8):1225–53.